

Title: Angular emission patterns of remnant black holes -- Towards a more complete temporal-spatial fitting with high precision

Speakers: Xiang Li

Series: Strong Gravity

Date: March 03, 2022 - 1:00 PM

URL: <https://pirsa.org/22030095>

Abstract: The gravitational radiation from the ringdown of a binary black hole merger is described by the solution of the Teukolsky equation, which predicts both the temporal and angular dependence of the emission. Many studies have explored the temporal feature of the ringdown wave through black hole spectroscopy. In this work, we further study the spatial distribution, by introducing a global fitting procedure over both temporal and spatial dependences, to propose a more complete test of General Relativity. We show that spin-weighted spheroidal harmonics are the better representation of the ringdown angular emission patterns compared to spin-weighted spherical harmonics. The differences are distinguishable in numerical relativity waveforms. We also study the correlation between progenitor binary properties and the excitation of quasinormal modes, including higher-order angular modes, overtones, prograde and retrograde modes. Specifically, we show that the excitation of retrograde modes is dominant when the remnant spin is anti-aligned with the binary orbital angular momentum. This study seeks to provide an analytical strategy and inspire the future development of ringdown test using real gravitational wave events.



Caltech



Australian
National
University

Angular emission patterns of remnant black holes

**Towards a more complete temporal-spatial fitting
with high precision**

Xiang Li (Caltech), and on behalf of
Ling (Lilli) Sun, Ka Lok (Rico) Lo, Ethan Payne, and Yanbei Chen.

Seminar talk at Strong Gravity Seminar at Perimeter Institute
2022 Mar. 3

Xiang Li (xiangli@caltech.edu)

1

Physical Review D 105 (2), 024016

Outline

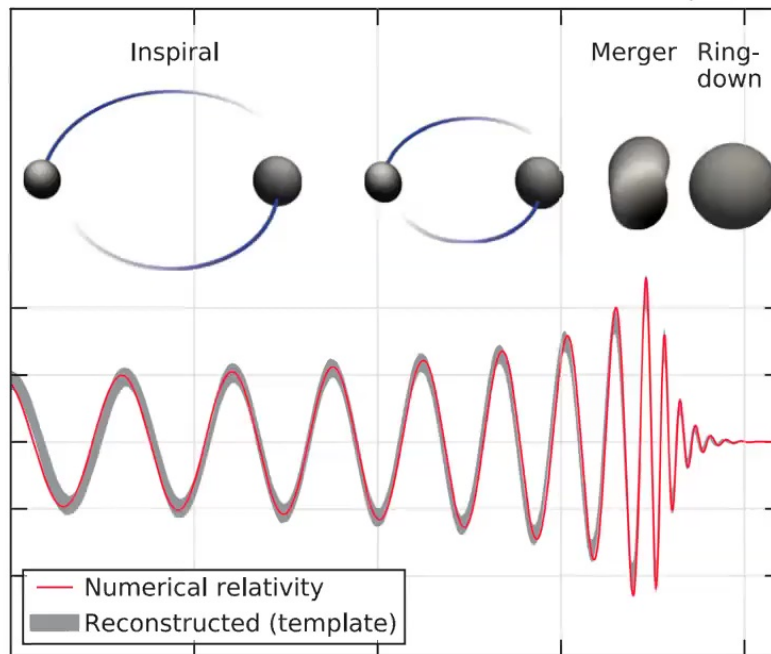
- Background and motivation
- Model and method
- Result
 - Benchmark binary G0
 - Nonspinning binaries
 - Spinning binaries
- Summary and outlook

Outline

- Background and motivation
- Model and method
- Result
 - Benchmark binary G0
 - Nonspinning binaries
 - Spinning binaries
- Summary and outlook

BBH ringdown stage

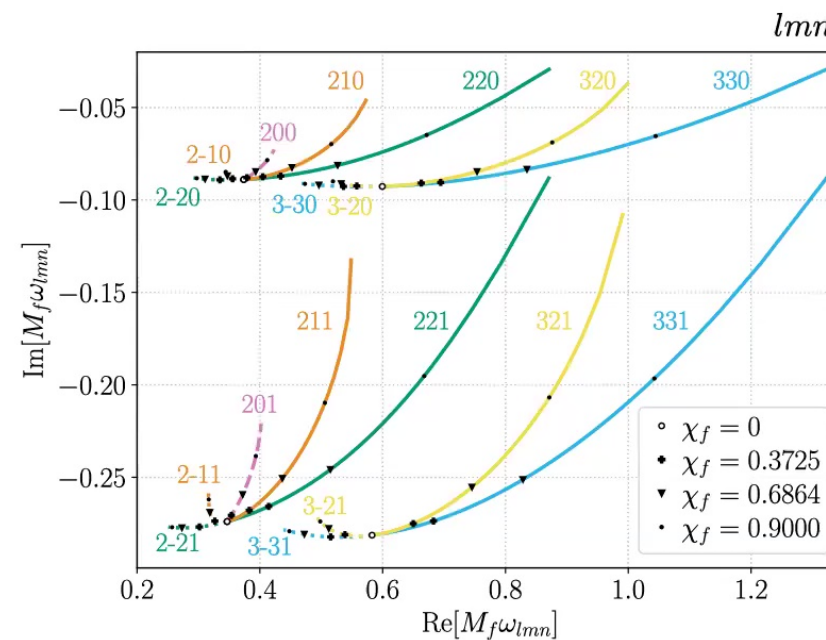
Abbott et al. PRL, 2016



TE temporal: QNM spectrum

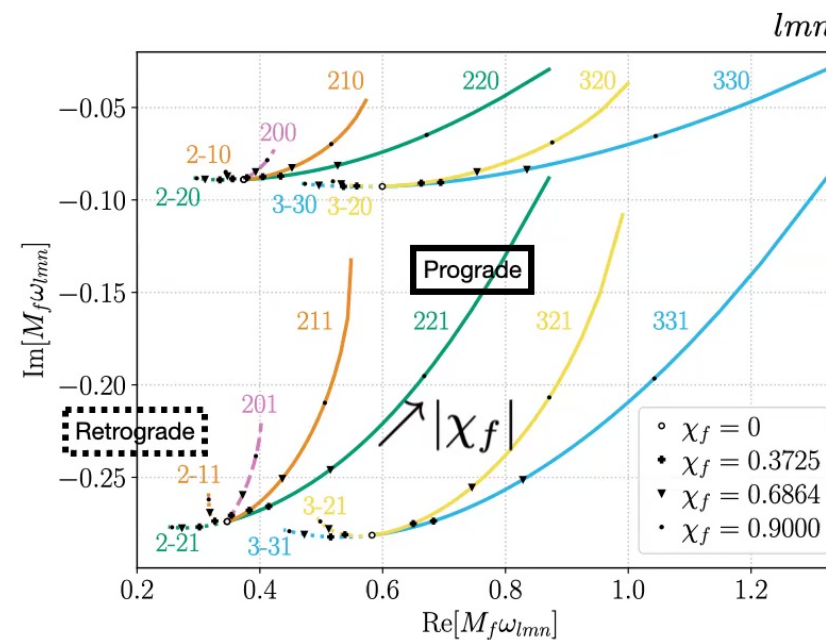
The complex QNM frequencies

$$\{\omega_{lmn}\}$$



TE temporal: QNM spectrum

The complex QNM frequencies
 $\{\omega_{lmn}\}$



TE temporal: QNM spectrum

The complex QNM frequencies

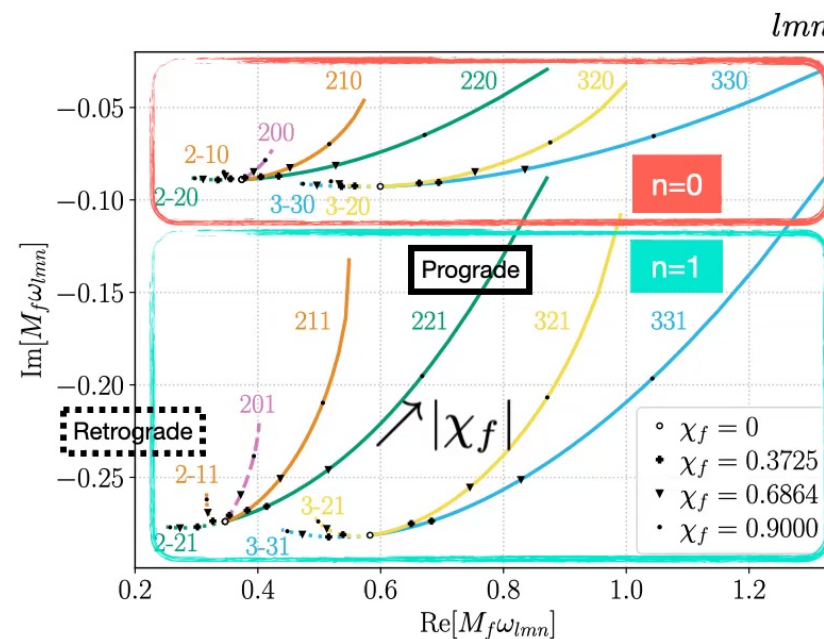
$$\{\omega_{lmn}\}$$

The no-hair theorem

$$\{M_f \quad a_f\}$$

Utilize overtones in fitting

(Giesler 2019 PRX)



Xiang Li (xiangli@caltech.edu)

5

Plot with `qnm` python package (Stein, L)

Spatial: spin-weighted spheroidal harmonics

- **Test of GR in ringdown stage**
 - *Spin-weighted spheroidal Harmonics*: black hole QNM
 - *Spin-weighted spherical Harmonics*: orthogonal & complete
 - *Mode mixing*: verification of theory & a future test of GR!!

$${}_{-2}S_{lm}(\gamma_{lmn}, \vec{\Omega}) = {}_{-2}Y_{lm}(\vec{\Omega}) + \gamma_{lmn} \sum_{l \neq l'} c_{l'lm} {}_{-2}Y_{l'm}(\vec{\Omega}) + \mathcal{O}(\gamma_{lmn})^2$$

Spheroidicity

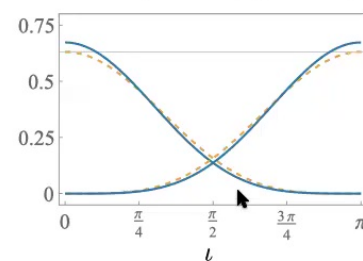
$$\gamma_{lmn} = \chi_f M_f \omega_{lmn}$$

Mixing coefficient

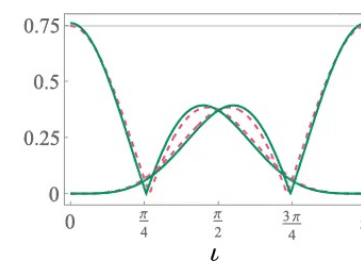
London, PRD, 2014

Spatial: spin-weighted spheroidal harmonics

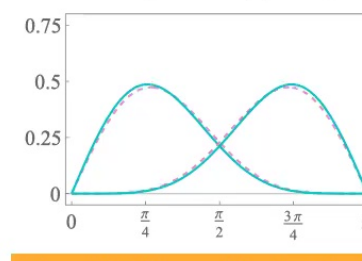
$$l = 2, m = 2, \gamma = 0.3$$



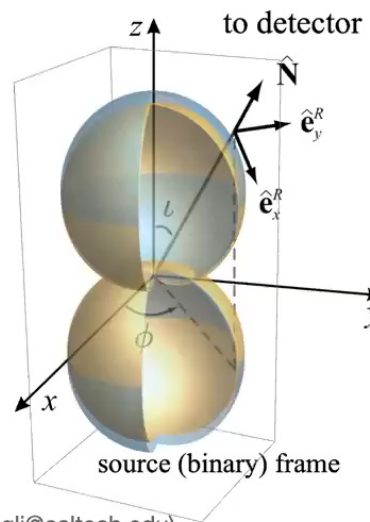
$$l = 3, m = 2, \gamma = 0.3$$



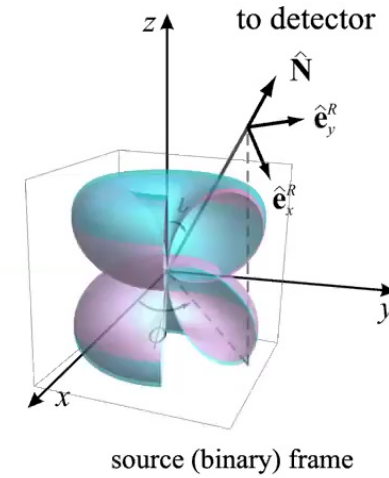
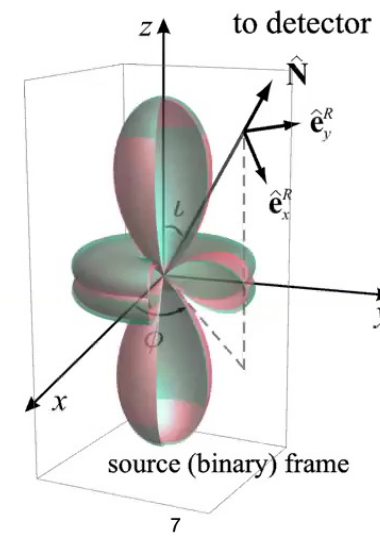
$$l = 3, m = 3, \gamma = 0.3$$



S: solid lines, Y: dashed lines



Xiang Li (xiangli@caltech.edu)

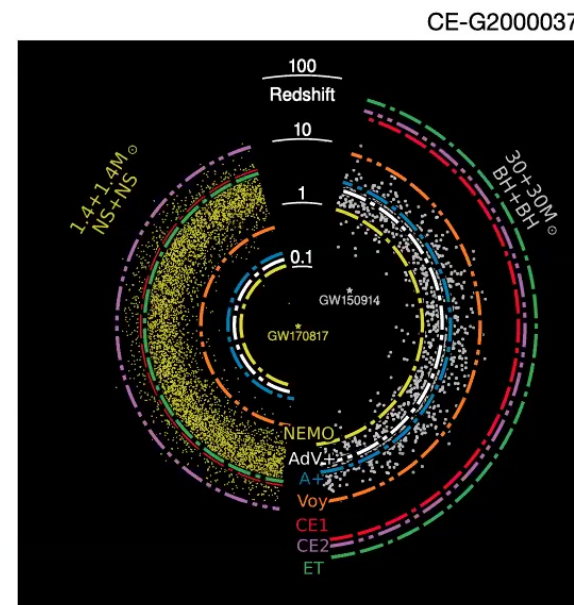
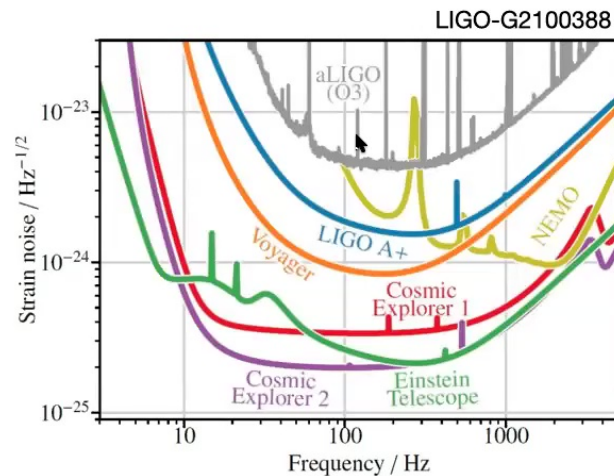


7

Future feasibility for ringdown test

Events with detectable HMs:

- GW190412 $(30.1, 8.3) M_{\odot}$, $q \approx 3.57$
- GW190521 $(85, 66) M_{\odot}$, $q \approx 1.27$
- GW190814 $(23.2, 2.59) M_{\odot}$, $q \approx 8.93$



Outline

- Background and motivation
- Model and method
- Result
 - Benchmark binary GO
 - Nonspinning binaries
 - Spinning binaries
- Summary and outlook

Ringdown waveform model

In final spin frame:

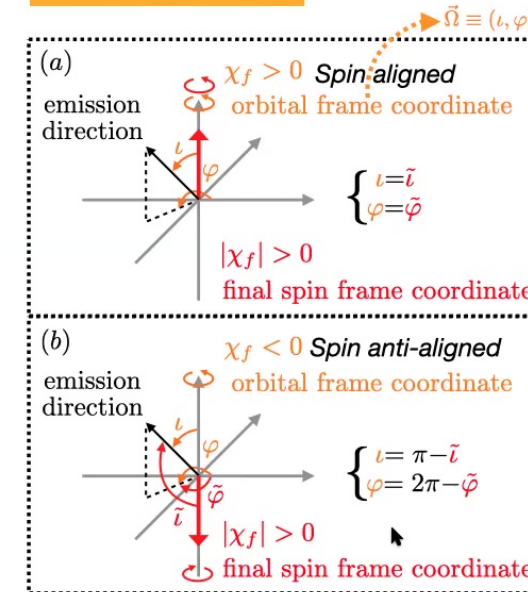
$$\begin{aligned}
 h^{(S)}(\tilde{\iota}, \tilde{\varphi}, t) &= (h_+ - i h_\times)^{(S)}(\tilde{\iota}, \tilde{\varphi}, t) \\
 &= \frac{M_f}{r} \sum_{l=2}^{l_{\max}} \sum_{m=-l}^l \sum_{n=0}^{n_{\max}} [B_{lmn}^{(S+)} e^{-i\omega_{lmn}(t-t_0)} -_2 S_{lm}(\gamma_{lmn}, \tilde{\iota}, \tilde{\varphi}) + \\
 &\quad B_{lmn}^{(S-)} e^{i\omega_{lmn}^*(t-t_0)} -_2 S_{lm}^*(\gamma_{lmn}, \pi - \tilde{\iota}, \tilde{\varphi})]
 \end{aligned}$$

S model

$$\begin{aligned}
 h^{(Y)}(\tilde{\iota}, \tilde{\varphi}, t) &= (h_+ - i h_\times)^{(Y)}(\tilde{\iota}, \tilde{\varphi}, t) \\
 &= \frac{M_f}{r} \sum_{l=2}^{l_{\max}} \sum_{m=-l}^l \sum_{n=0}^{n_{\max}} [B_{lmn}^{(Y+)} e^{-i\omega_{lmn}(t-t_0)} -_2 Y_{lm}(\tilde{\iota}, \tilde{\varphi}) + \\
 &\quad B_{lmn}^{(Y-)} e^{i\omega_{lmn}^*(t-t_0)} -_2 Y_{lm}^*(\pi - \tilde{\iota}, \tilde{\varphi})]
 \end{aligned}$$

Y model

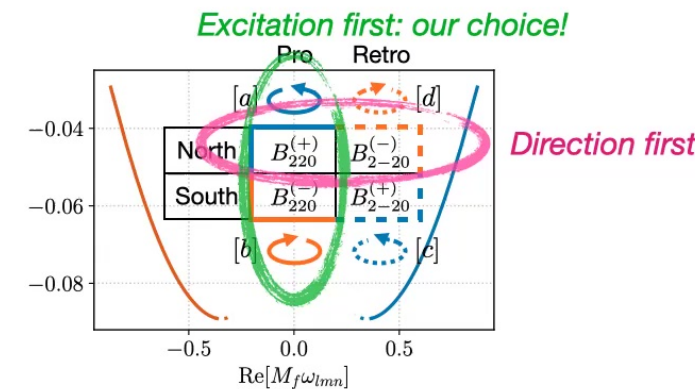
In orbital frame:



Conventions of QNM expansion

In final spin frame:

$$\begin{aligned} h^{(S)}(\tilde{\iota}, \tilde{\varphi}, t) &= (h_+ - i h_\times)^{(S)}(\tilde{\iota}, \tilde{\varphi}, t) \\ &= \frac{M_f}{r} \sum_{l=2}^{l_{\max}} \sum_{m=-l}^l \sum_{n=0}^{n_{\max}} [B_{lmn}^{(S+)} e^{-i\omega_{lmn}(t-t_0)} {}_2S_{lm}(\gamma_{lmn}, \tilde{\iota}, \tilde{\varphi}) + \\ &\quad B_{lmn}^{(S-)} e^{i\omega_{lmn}^*(t-t_0)} {}_2S_{lm}^*(\gamma_{lmn}, \pi - \tilde{\iota}, \tilde{\varphi})] \end{aligned}$$



$$h(t, r, \tilde{\iota}, \tilde{\varphi}) = \frac{M_f}{r} \sum_{l=2}^{l_{\max}} \sum_{m=-l}^l \sum_{n=0}^{n_{\max}} \left[\underbrace{A_{lmn}^R e^{-i\omega_{lmn}(t-r^*)} {}_2S_{lmn}(\chi_f M_f \omega_{lmn}, \tilde{\iota}, \tilde{\varphi})}_{[a] \text{ for } m>0; [c] \text{ for } m<0;} + \underbrace{A_{lmn}^L e^{i\omega_{lmn}^*(t-r^*)} {}_2S_{lmn}(-\chi_f M_f \omega_{lmn}^*, \tilde{\iota}, \tilde{\varphi})}_{[d] \text{ for } m>0; [b] \text{ for } m<0.} \right]$$

$m \rightarrow -m$

$$h(t, r, \tilde{\iota}, \tilde{\varphi}) = \frac{M_f}{r} \sum_{l=2}^{l_{\max}} \sum_{m=-l}^l \sum_{n=0}^{n_{\max}} \left[\underbrace{A_{lmn}^{(+)} e^{-i\omega_{lmn}(t-r^*)} {}_2S_{lmn}(\chi_f M_f \omega_{lmn}, \tilde{\iota}, \tilde{\varphi})}_{[a] \text{ for } m>0; [c] \text{ for } m<0;} + \underbrace{A_{lmn}^{(-)} e^{i\omega_{lmn}^*(t-r^*)} {}_2S_{lmn}^*(\chi_f M_f \omega_{lmn}, \pi - \tilde{\iota}, \tilde{\varphi})}_{[b] \text{ for } m>0; [d] \text{ for } m<0.} \right]$$

Conventions of QNM expansion

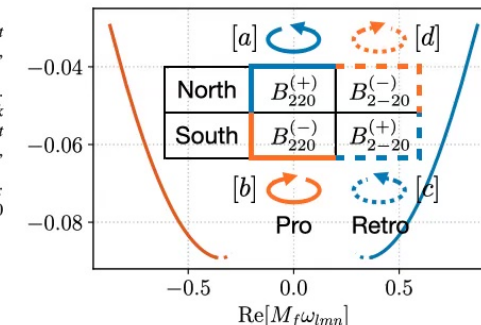
	[a]	[b]	[c]	[d]
Temporal-spatial profile	$e^{-i\omega_{220}t} {}_{-2}S_{220}(\gamma_{220}, \tilde{t}, \tilde{\varphi})$	$e^{i\omega_{220}^* t} {}_{-2}S_{220}^*(\gamma_{220}, \pi - \tilde{t}, \tilde{\varphi})$	$e^{-i\omega_{2-20}t} {}_{-2}S_{2-20}(\gamma_{2-20}, \tilde{t}, \tilde{\varphi})$	$e^{i\omega_{2-20}^* t} {}_{-2}S_{2-20}^*(\gamma_{2-20}, \pi - \tilde{t}, \tilde{\varphi})$
Amplitude in our expression	$B_{220}^{(+)}$	$B_{220}^{(-)}$	$B_{2-20}^{(+)}$	$B_{2-20}^{(-)}$
Right/Left-handed (R/L)	R	L	R	L
Prograde/Retrograde	Prograde	Prograde	Retrograde	Retrograde
Emission direction (in final spin frame)	North	South	South	North
Angular eigenfunction (standard form)	${}_{-2}S_{220}(\gamma_{220}, \tilde{t}, \tilde{\varphi})$	${}_{-2}S_{2-20}(-\gamma_{220}^*, \tilde{t}, \tilde{\varphi})$	${}_{-2}S_{2-20}(\gamma_{2-20}, \tilde{t}, \tilde{\varphi})$	${}_{-2}S_{220}(-\gamma_{2-20}^*, \tilde{t}, \tilde{\varphi})$
Amplitude in [2] ^a (2006)	\mathcal{A}_{220}	\mathcal{A}'_{220} (mirror mode of [a])	\mathcal{A}_{2-20}	\mathcal{A}'_{2-20} (mirror mode of [c])
Terminology in [9] (2014)	Regular mode	Regular mode	Mirror mode of [b]	Mirror mode of [a]
Amplitude in [6, 8] (2019)	\mathcal{A}_{220}	\mathcal{A}'_{220}	\mathcal{A}_{2-20}	\mathcal{A}'_{2-20}
Amplitude in [1] (2021)	\mathcal{A}_{220}	\mathcal{A}_{2-20}	(not included)	(not included)
Amplitude in [7] (2021)	$C_{[1]220}$	C'_{2-20} (mirror mode of [c])	$C_{[-1]220}$	C'_{220} (mirror mode of [a])
Amplitude in [5] (2021)	C_{220}	C_{2-20}	C_{2-20}	C'_{220} (mirror mode of [a])
Amplitude in [3, 4] (2021)	C_{220}	C_{2-20}	C'_{2-20} (mirror mode of [b])	C'_{220} (mirror mode of [a])

^a Ref. [2] denotes GW strain tensor as $h_+ + i h_\times$, thus we include a sign change in angular frequency when comparing the convention in [2] with other papers.

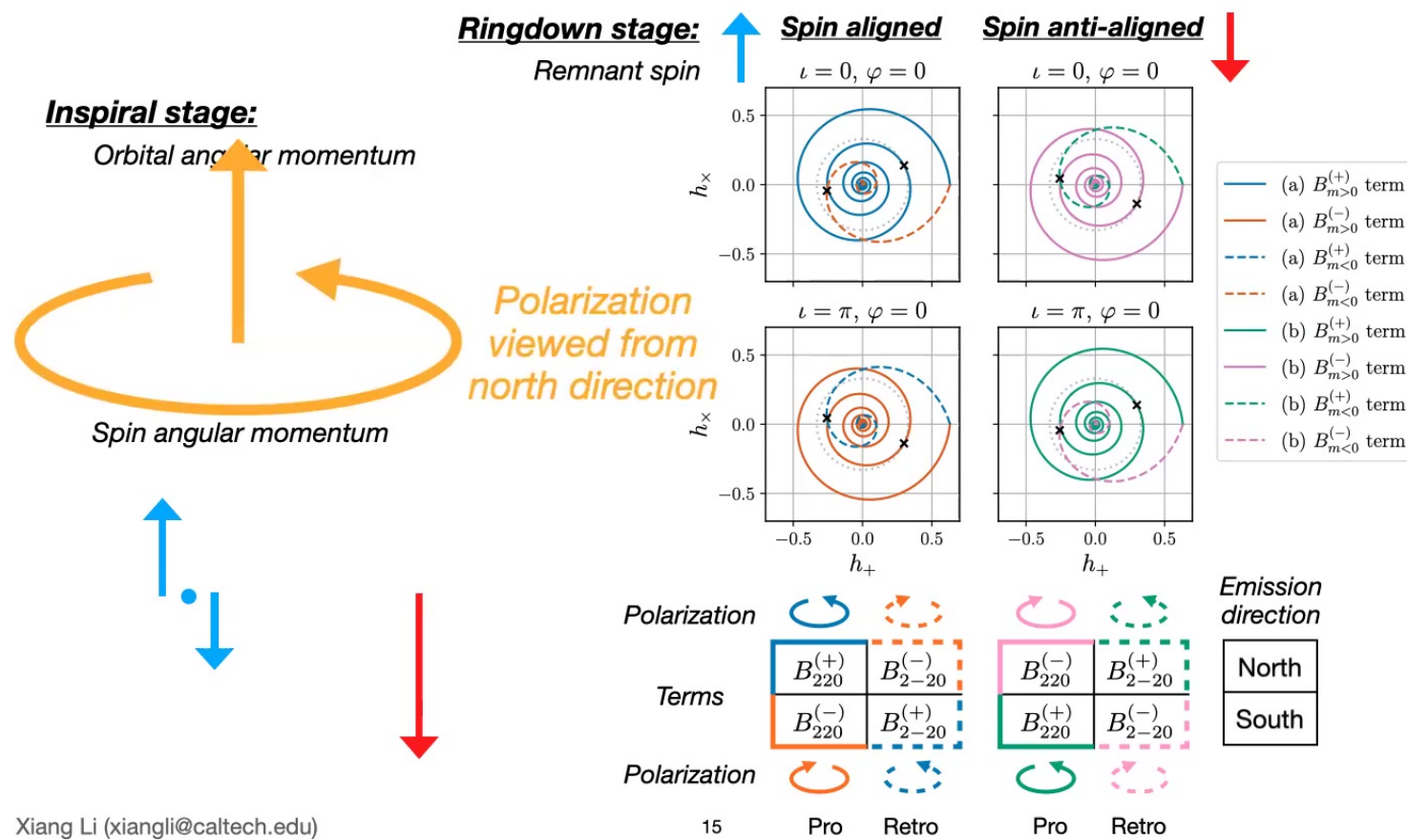
- [1] R. ABBOTT ET AL., *Tests of General Relativity with Binary Black Holes from the second LIGO-Virgo Gravitational-Wave Transient Catalog*, 10 2020.
- [2] E. BERTI, V. CARDOSO, AND C. M. WILL, *Gravitational-wave spectroscopy of massive black holes with the space interferometer LISA*, Phys. Rev. D, 73 (2006), p. 064030.
- [3] A. DHANI, *Importance of mirror modes in binary black hole ringdown waveform*, Phys. Rev. D, 103 (2021), p. 104048.
- [4] A. DHANI AND B. S. SATHYAPRAKASH, *Overtones, mirror modes, and mode-mixing in binary black hole mergers*, 7 2021.
- [5] E. FINCH AND C. J. MOORE, *Modelling the ringdown from precessing black hole binaries*, 2021.
- [6] S. A. HUGHES, A. APTE, G. KHANNA, AND H. LIM, *Learning about black hole binaries from their ringdown spectra*, Phys. Rev. Lett., 123 (2019), p. 161101.
- [7] M. ISI AND W. M. FARR, *Analyzing black-hole ringdowns*, 7 2021.
- [8] H. LIM, G. KHANNA, A. APTE, AND S. A. HUGHES, *Exciting black hole modes via misaligned coalescences: II. The mode content of late-time coalescence waveforms*, Phys. Rev. D, 100 (2019), p. 084032.
- [9] L. LONDON, D. SHOEMAKER, AND J. HEALY, *Modeling ringdown: Beyond the fundamental quasinormal modes*, Phys. Rev. D, 90 (2014), p. 124032. [Erratum: Phys. Rev. D 94, 069902 (2016)].

Xiang Li (xiangli@caltech.edu)

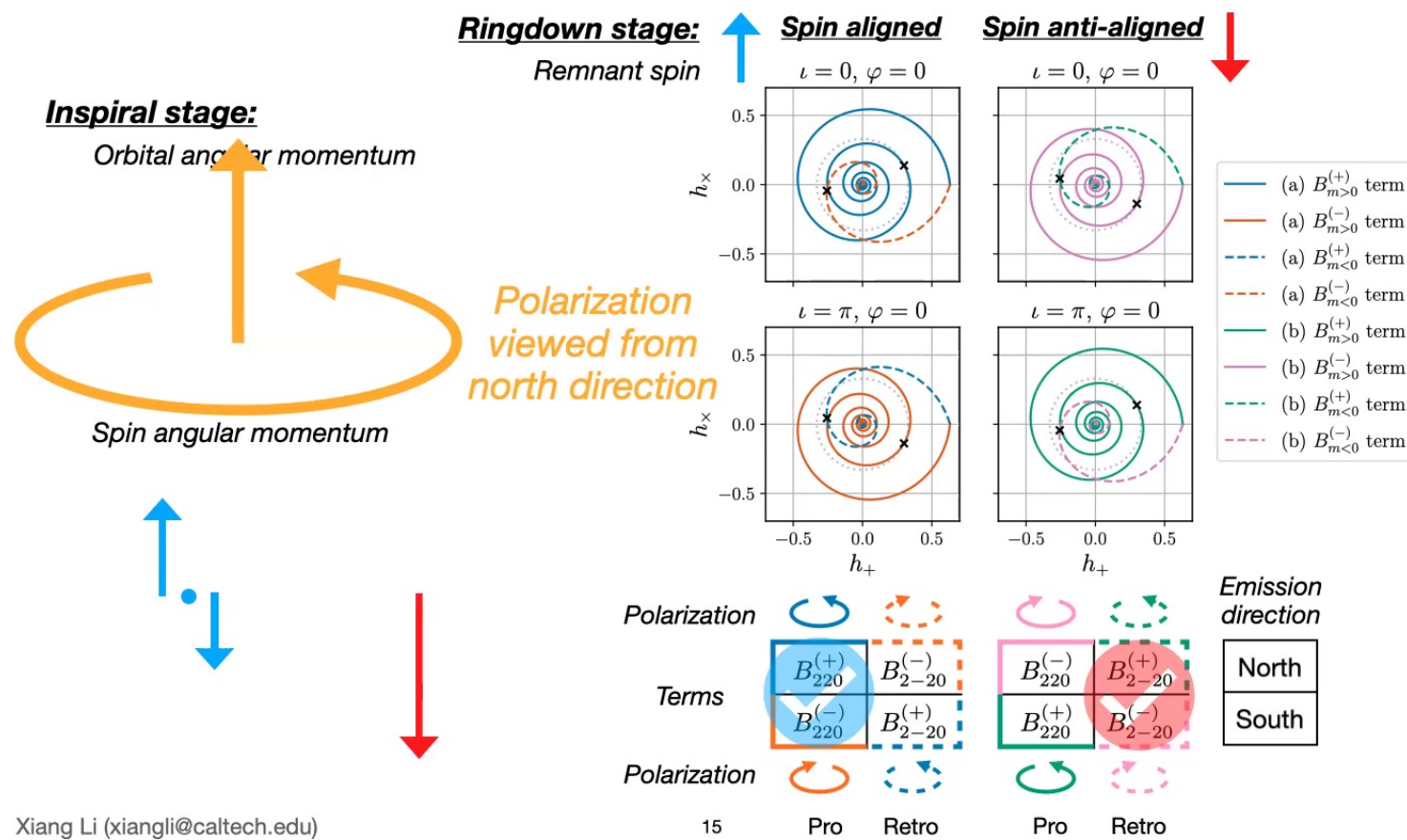
12



Continuity from inspiral to ringdown



Continuity from inspiral to ringdown



Spatial-temporal fitting strategy

Target waveforms and templates

$$h(\vec{\Omega}, t) = \sum_{lm} {}_{-2}Y_{lm}(\vec{\Omega}) h_{lm}(t)$$

From SXS

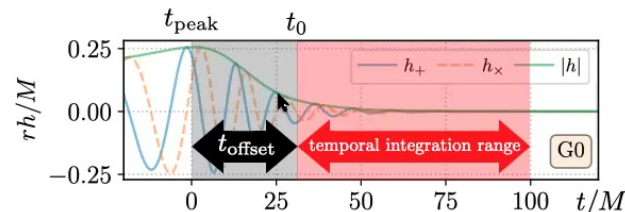
$$g(\vec{\Omega}, t) = (h_+ - i h_\times)^{(S/Y)}(\vec{\Omega}, t)$$

In the linear space w/ coord $\{B_{lmn}^{(S/Y\pm)}|lmn\}$

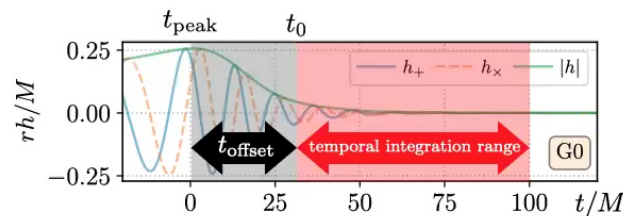
Temporal-spatial inner product

$$\langle g | h \rangle = \int d\vec{\Omega} \int_{t_0}^{+\infty} dt [g^*(\vec{\Omega}, t) h(\vec{\Omega}, t)]$$

Truncated starting time



Spatial-temporal fitting strategy



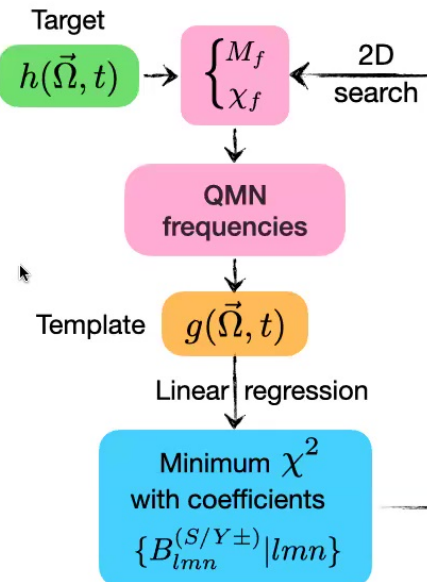
Parameter dependencies

Hyperparameter: t_0

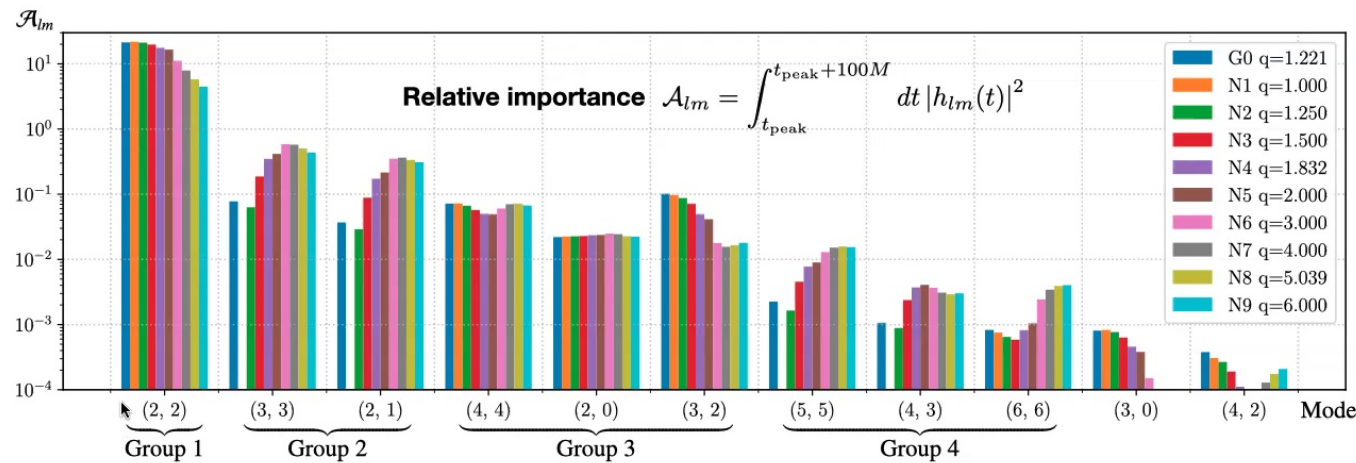
Intrinsic: (M_f, χ_f)

Coefficients: $\{B_{lmn}^{(S/Y\pm)}|lmn\}$

Strategy for minimizing distance



Spatial-temporal fitting strategy

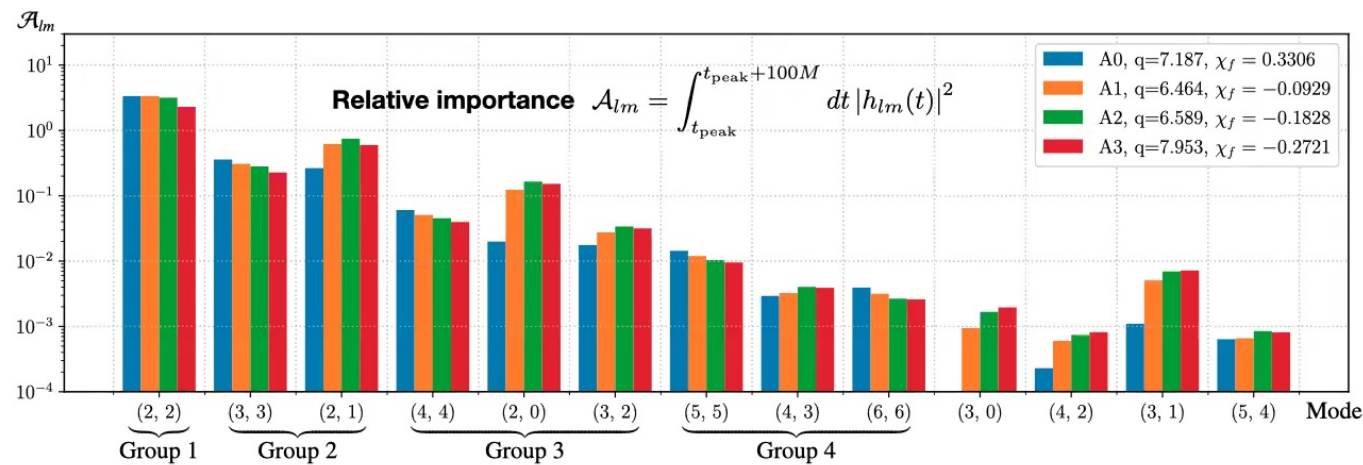


Strategy for adding (l,m) modes

Group 1: (2, 2),
 Group 2: (3, 3), (2, 1),
 Group 3: (4, 4), (2, 0), (3, 2),
 Group 4: (5, 5), (4, 3), (6, 6).

Label	SXSID/Lev	q_{ref}	χ_{eff}	χ_f
G0	0305/Lev6	1.221	-0.0166	0.6921
N1	1154/Lev3	1.000	0.0000	0.6864
N2	1143/Lev3	1.250	-0.0001	0.6795
N3	0593/Lev3	1.500	0.0001	0.6641
N4	1354/Lev3	1.832	-0.0001	0.6377
N5	1166/Lev3	2.000	0.0000	0.6234
N6	2265/Lev3	3.000	0.0000	0.5406
N7	1906/Lev3	4.000	0.0000	0.4718
N8	0187/Lev3	5.039	0.0000	0.4148
N9	0181/Lev4	6.000	-0.0000	0.3725

Spatial-temporal fitting strategy



Strategy for adding (l,m) modes

- Group 1: (2, 2),
- Group 2: (3, 3), (2, 1),
- Group 3: (4, 4), (2, 0), (3, 2),

Label	SXSID/Lev	q_{ref}	χ_{eff}	χ_f
A0	0188/Lev3	7.187	-0.0000	0.3306
A1	1424/Lev3	6.464	-0.6757	-0.0929
A2	1435/Lev3	6.589	-0.6764	-0.1828
A3	1422/Lev3	7.953	-0.7620	-0.2721

Outline

- Background and motivation
- Model and method
- **Result**
 - Benchmark binary GO
 - Nonspinning binaries
 - Spinning binaries
- Summary and outlook

→

Motivation

Method

Result

Outlook

Result of binary G0

Label	SXSID/Lev	q_{ref}	χ_{eff}	χ_f
G0	0305/Lev6	1.221	-0.0166	0.6921
N1	1154/Lev3	1.000	0.0000	0.6864
N2	1143/Lev3	1.250	-0.0001	0.6795
N3	0593/Lev3	1.500	0.0001	0.6641
N4	1354/Lev3	1.832	-0.0001	0.6377
N5	1166/Lev3	2.000	0.0000	0.6234
N6	2265/Lev3	3.000	0.0000	0.5406
N7	1906/Lev3	4.000	0.0000	0.4718
N8	0187/Lev3	5.039	0.0000	0.4148
N9	0181/Lev4	6.000	-0.0000	0.3725

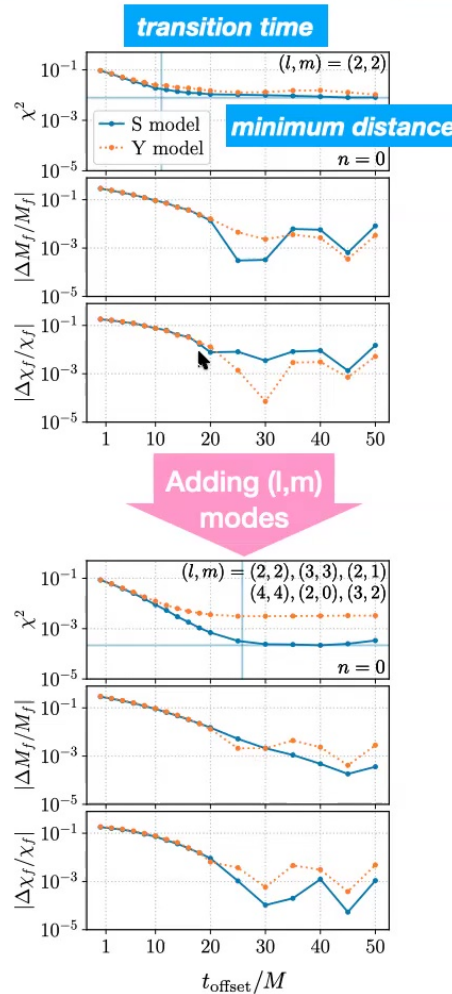


Motivation

Method

Result

Outlook

Result of binary G0

Xiang Li (xiangli@caltech.edu)

Label	SXSID/Lev	q_{ref}	χ_{eff}	χ_f
G0	0305/Lev6	1.221	-0.0166	0.6921
N1	1154/Lev3	1.000	0.0000	0.6864
N2	1143/Lev3	1.250	-0.0001	0.6795
N3	0593/Lev3	1.500	0.0001	0.6641
N4	1354/Lev3	1.832	-0.0001	0.6377
N5	1166/Lev3	2.000	0.0000	0.6234
N6	2265/Lev3	3.000	0.0000	0.5406
N7	1906/Lev3	4.000	0.0000	0.4718
N8	0187/Lev3	5.039	0.0000	0.4148
N9	0181/Lev4	6.000	-0.0000	0.3725

Motivation

Method

Result

Outlook

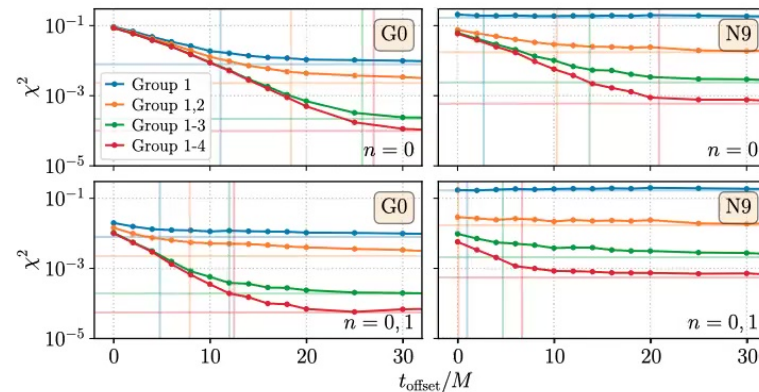
Result of binary G0

Xiang Li (xiangli@caltech.edu)

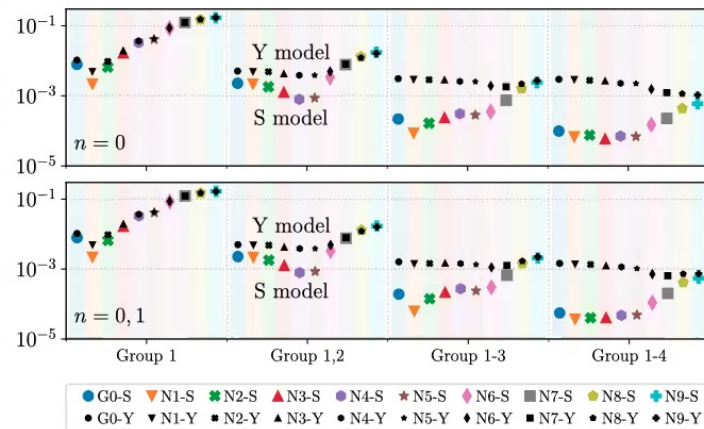
22

Nonspinning summarizing plots

Example result: G0 and N9 (S model)



Summarizing plot: minimum distance



Spatial-temporal fitting strategy

Spatial-temporal fitting strategy

Target waveforms and templates

$$h(\vec{\Omega}, t) = \sum_{lm} {}_{-2}Y_{lm}(\vec{\Omega}) h_{lm}(t)$$

From SXS

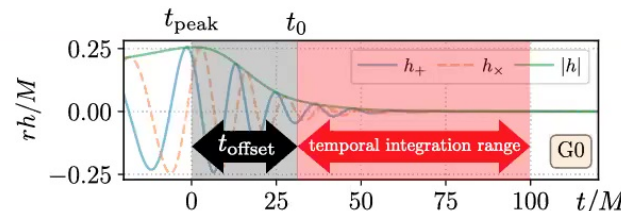
$$g(\vec{\Omega}, t) = (h_+ - i h_\times)^{(S/Y)}(\vec{\Omega}, t)$$

In the linear space w/ coord $\{B_{lmn}^{(S/Y\pm)}|lmn\}$

Temporal-spatial inner product

$$\langle g | h \rangle = \int d\vec{\Omega} \int_{t_0}^{+\infty} dt [g^*(\vec{\Omega}, t) h(\vec{\Omega}, t)]$$

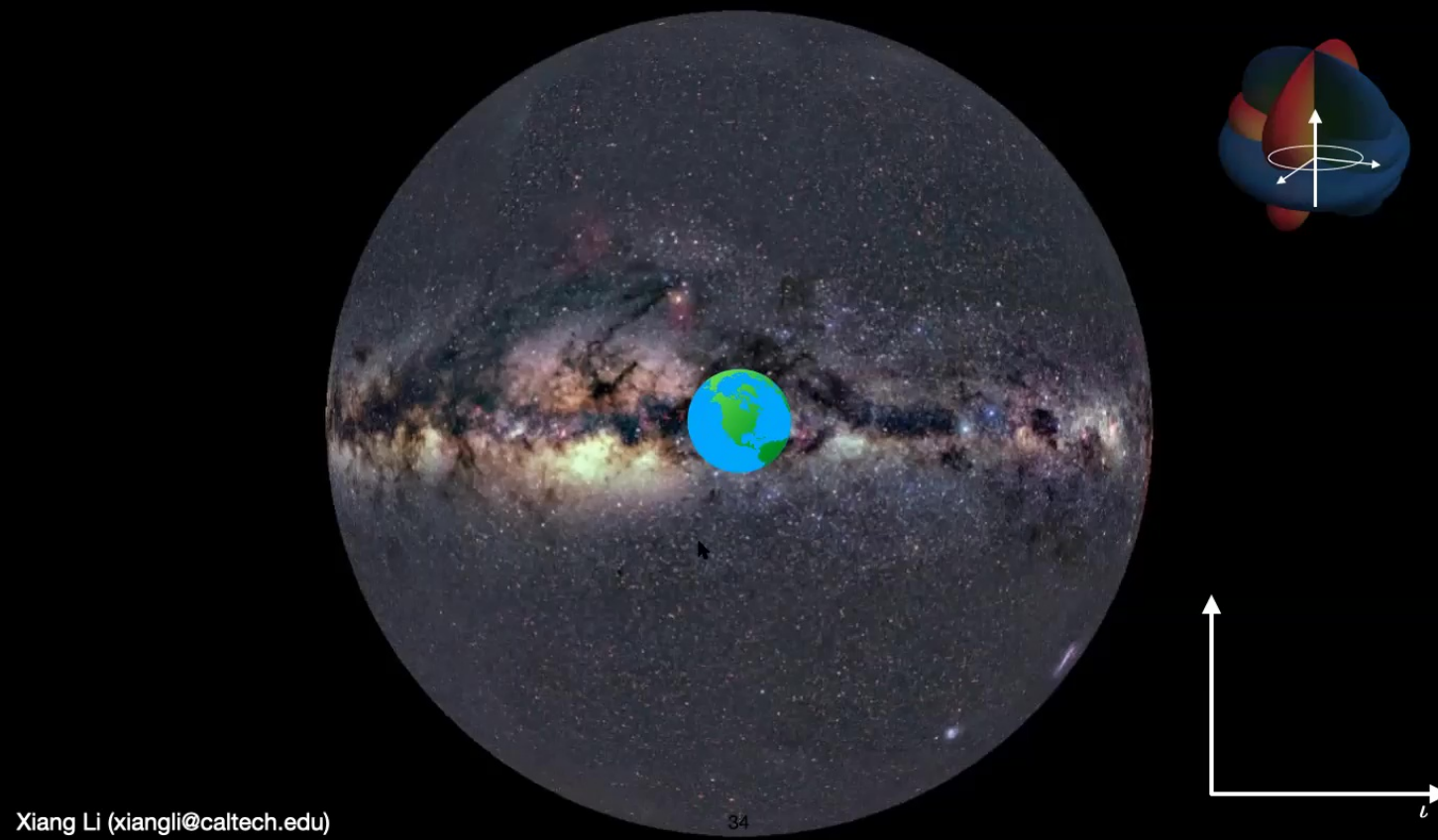
Truncated starting time



Distance in the linear space

$$\chi^2[h, g] = \frac{\langle h - g | h - g \rangle}{\langle h | h \rangle}$$

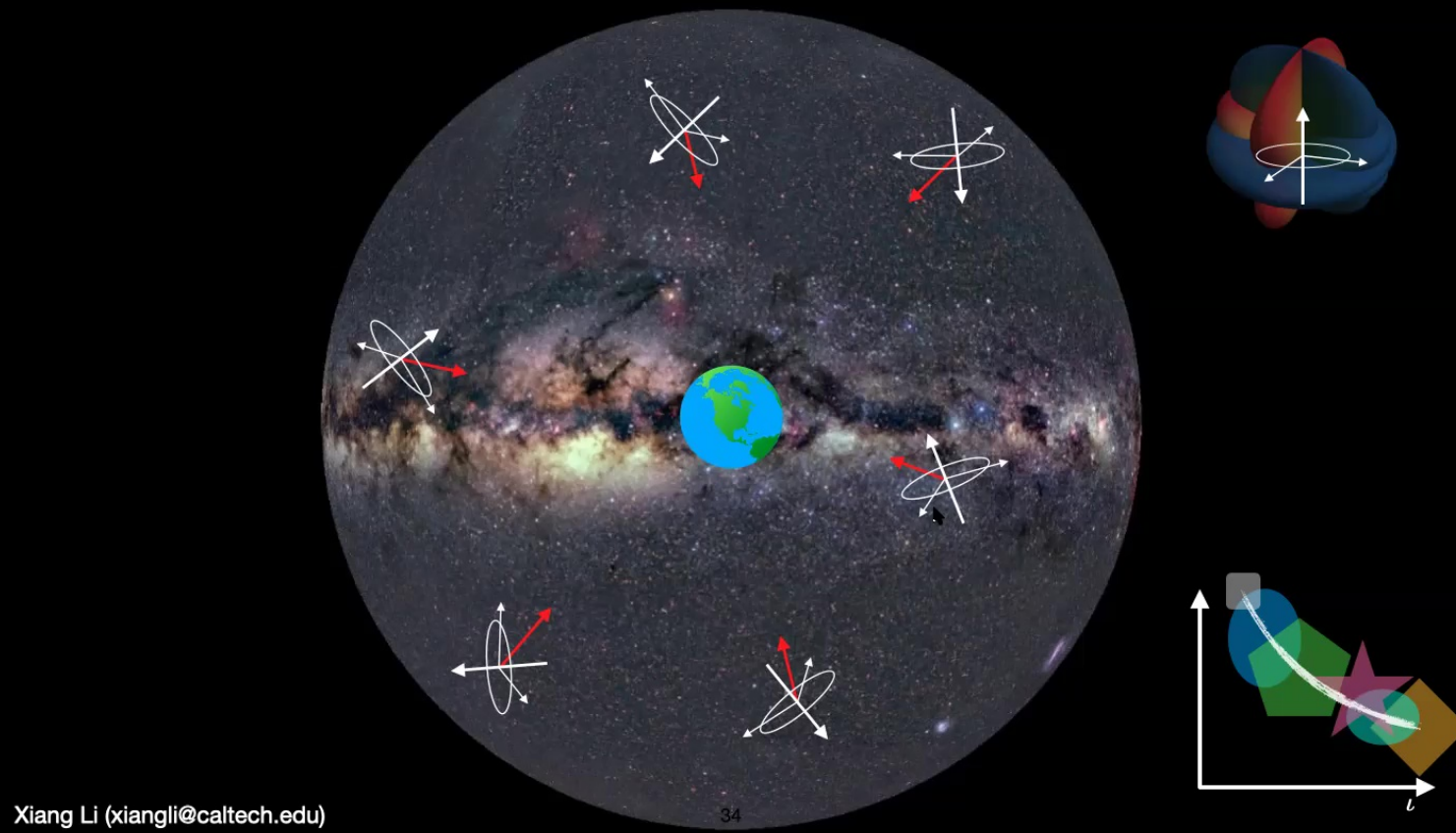
Future waveform stacking strategy



Xiang Li (xiangli@caltech.edu)

34

Future waveform stacking strategy

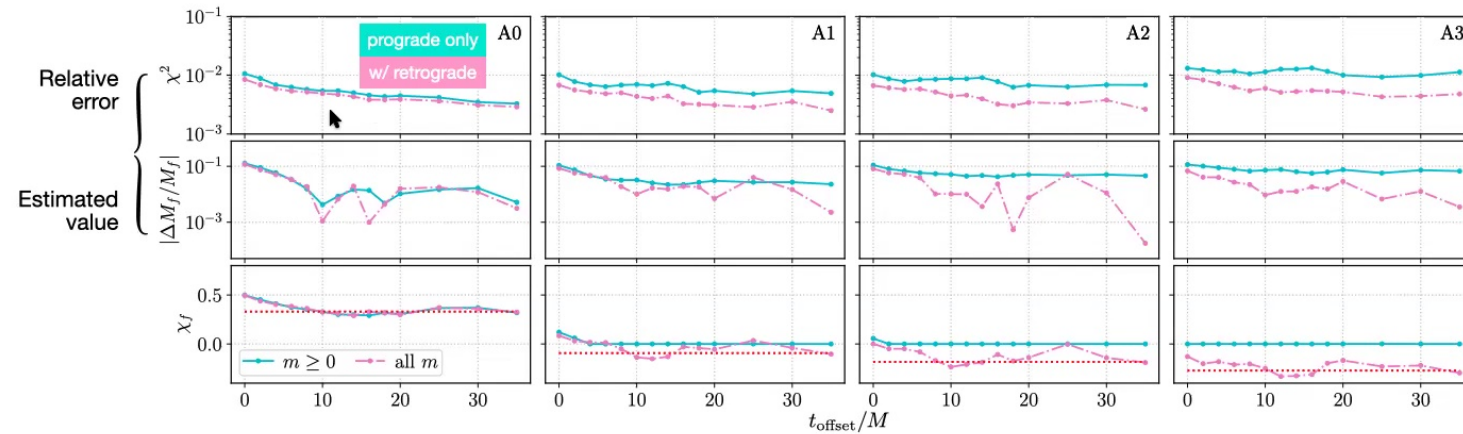


Result analysis I

- S/Y model distinguishability
 - S model win!
 - Smaller q case wins more
- Higher order angular modes
 - reduce the minimum distance
 - enlarge S/Y model distinguishability
 - larger q binaries benefit more
- Higher order overtones
 - bring the transition time earlier
 - maintain S/Y model distinguishability

Result of spinning binaries

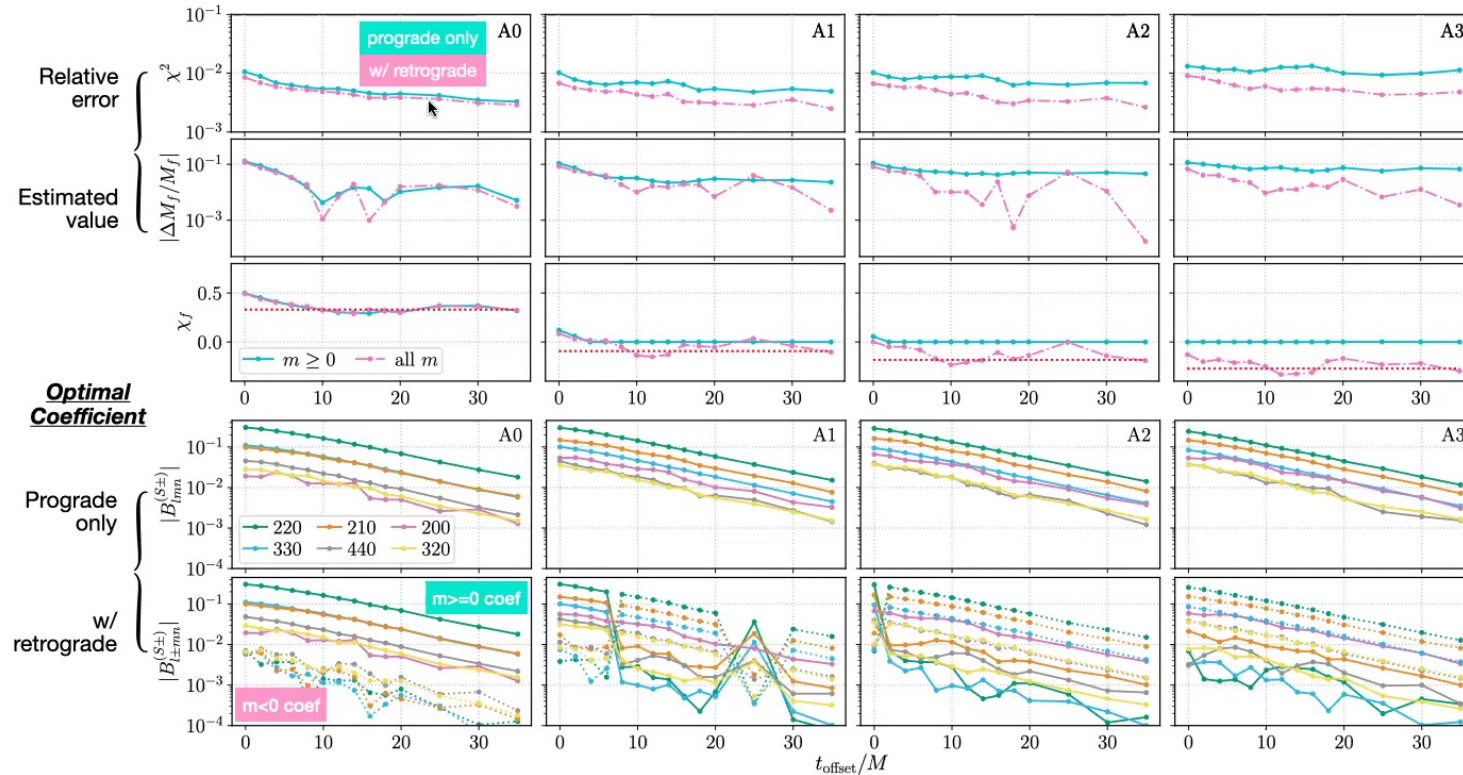
Fitting Results w/ Group 1–3



Label	SXSID/Lev	q_{ref}	χ_{eff}	χ_f
A0	0188/Lev3	7.187	-0.0000	0.3306
A1	1424/Lev3	6.464	-0.6757	-0.0929
A2	1435/Lev3	6.589	-0.6764	-0.1828
A3	1422/Lev3	7.953	-0.7620	-0.2721

Result of spinning binaries

Fitting Results w/ Group 1–3

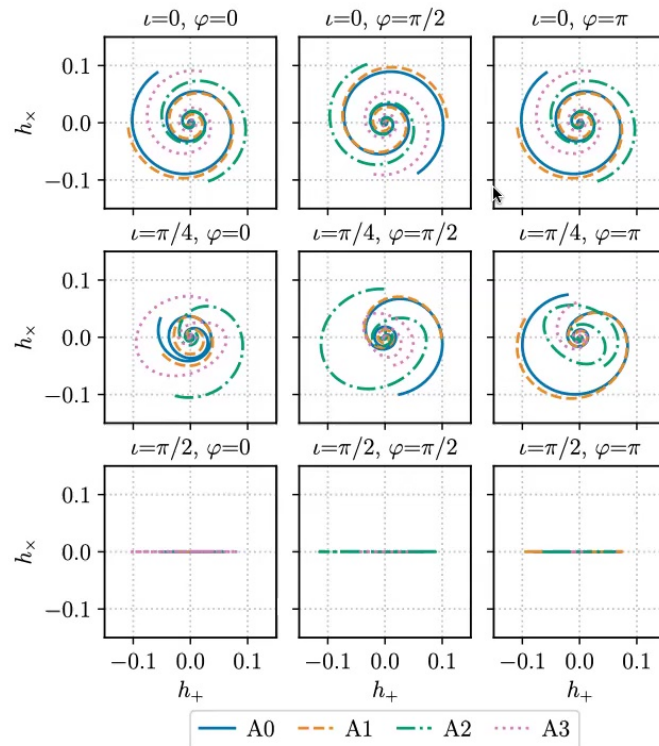


Xiang Li (xiangli@caltech.edu)

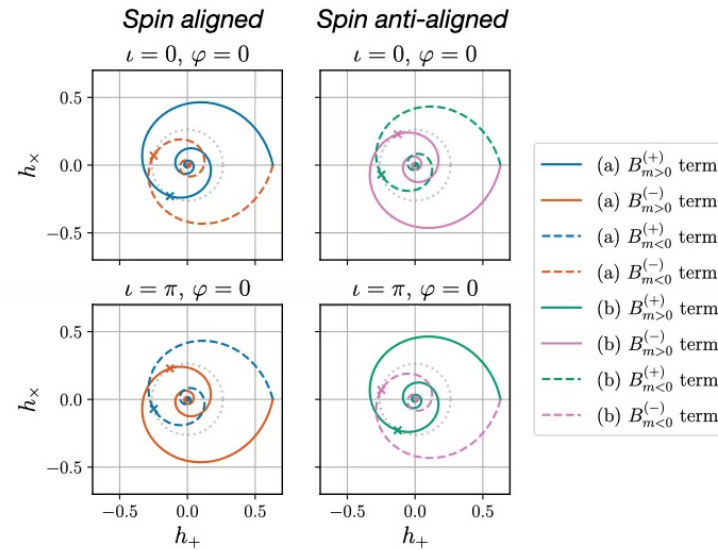
26

Result analysis II – spatial

Data polarization pattern



Model polarization pattern



$$h^{(S)}(\tilde{\iota}, \tilde{\varphi}, t) = (h_+ - i h_x)^{(S)}(\tilde{\iota}, \tilde{\varphi}, t)$$

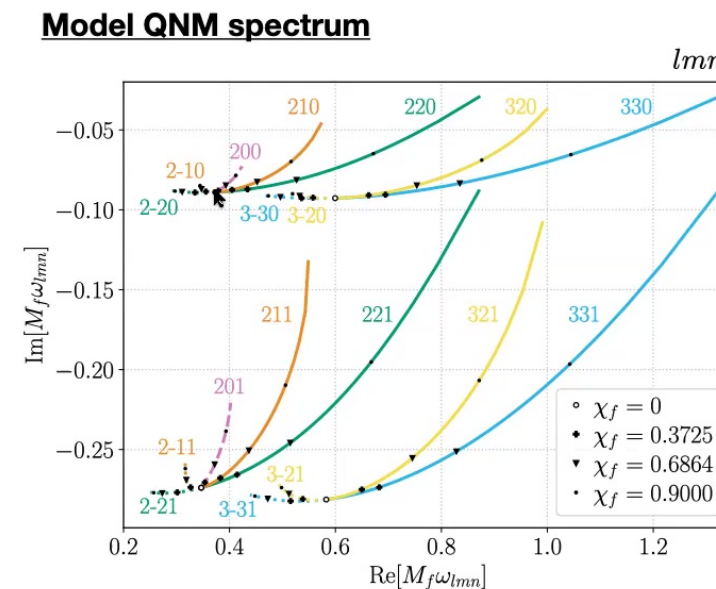
$$= \frac{M_f}{r} \sum_{l=2}^{l_{\max}} \sum_{m=-l}^{m=l} \sum_{n=0}^{n_{\max}} [B_{lmn}^{(S+)} e^{-i\omega_{lmn}(t-t_0)} {}_{-2}S_{lm}(\gamma_{lmn}, \tilde{\iota}, \tilde{\varphi}) + \\ B_{lmn}^{(S-)} e^{i\omega_{lmn}^*(t-t_0)} {}_{-2}S_{lm}^*(\gamma_{lmn}, \pi - \tilde{\iota}, \tilde{\varphi})]$$

S model

Xiang Li (xiangli@caltech.edu)

Result analysis II – temporal

- Retrograde excitations
 - Important in spin anti-aligned case!
 - More significant in larger spin case.



Xiang Li (xiangli@caltech.edu)

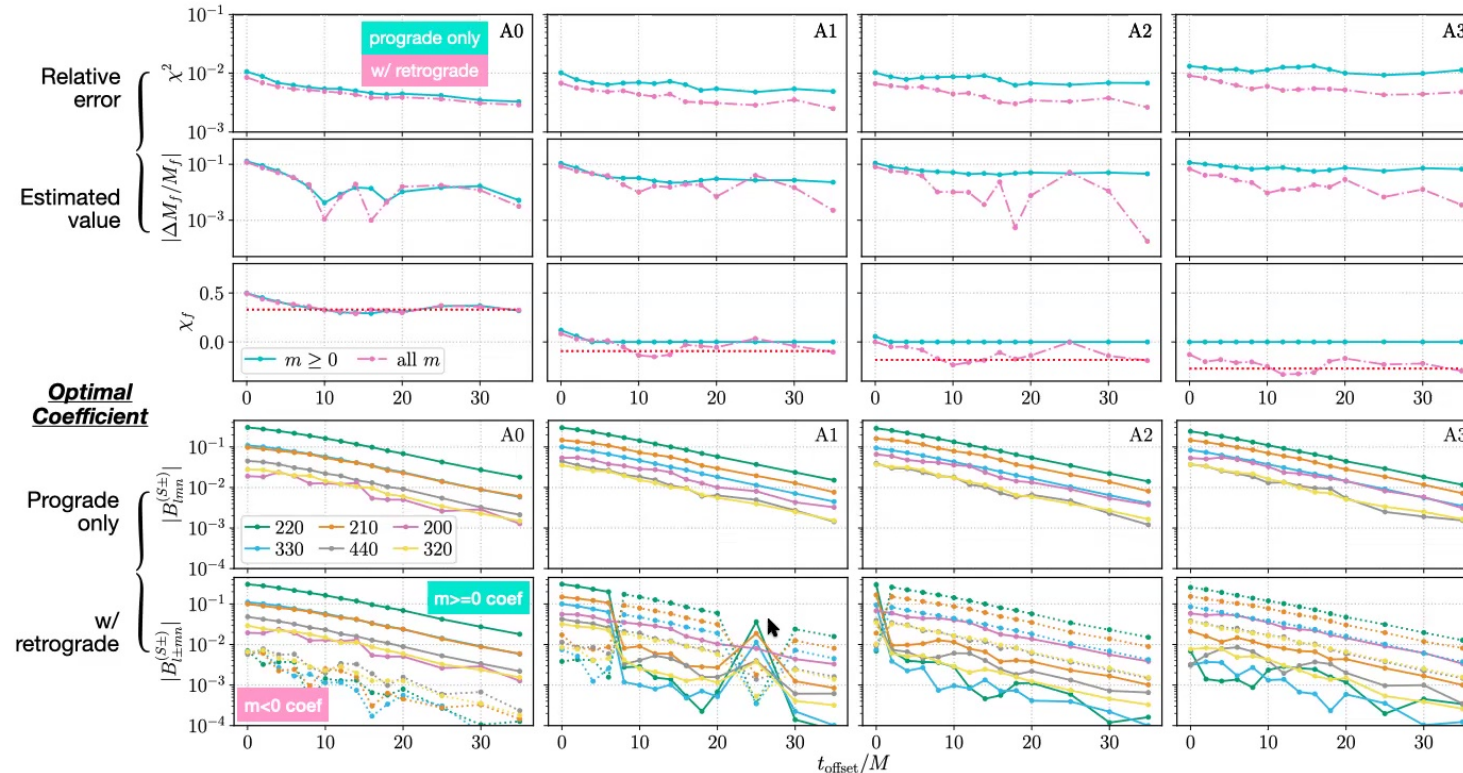
28

Plot with `qnm` python package (Stein, L)

Label	χ_f
A0	0.3306
A1	-0.0929
A2	-0.1828
A3	-0.2721

Result of spinning binaries

Fitting Results w/ Group 1–3



Xiang Li (xiangli@caltech.edu)

29

Outline

- Background
- Model and method
- Result
 - Benchmark binary GO
 - Nonspinning binaries
 - Spinning binaries
- Summary and outlook

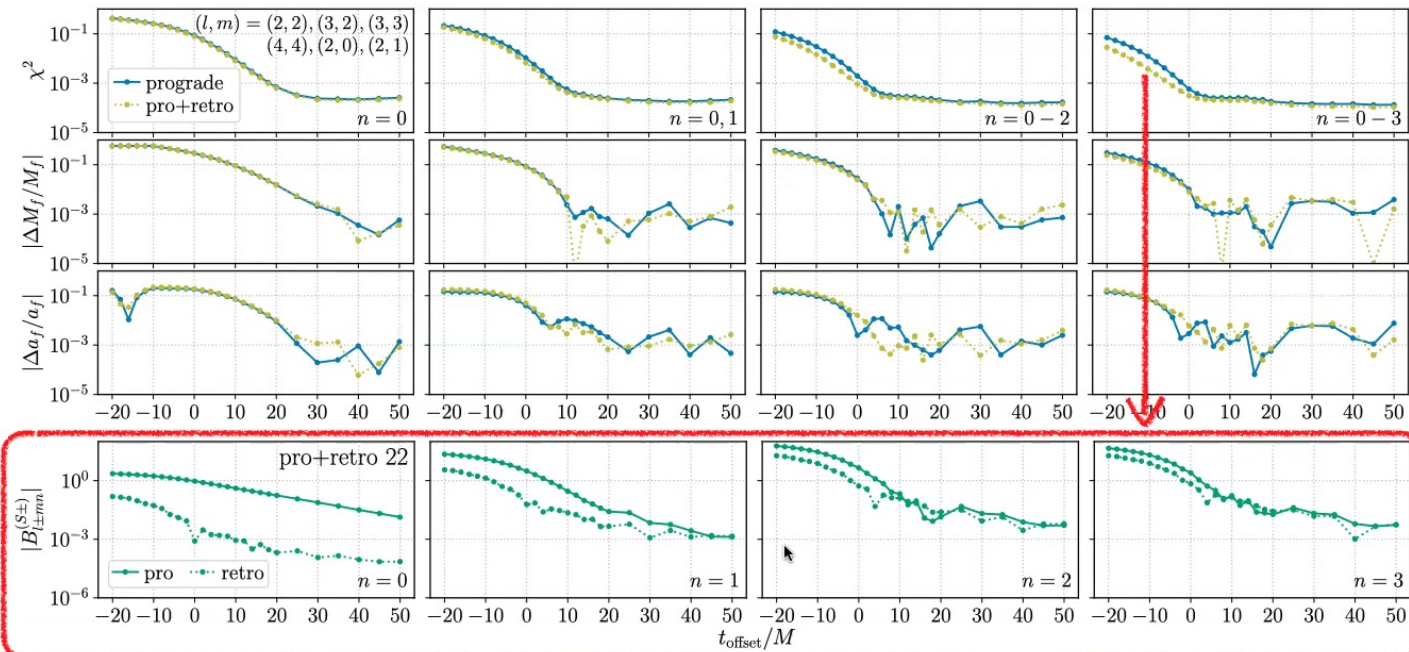
Summary and outlook

- Towards a more complete test of GR
 - QNM temporal-spatial fitting
 - S/Y distinguishability
 - Retrograde excitations
- BH spectroscopy conclusions reinforced
 - Higher-order (l,m) modes
 - Overtones
- **Outlook**
 - Spin misaligned cases? Mass/current quadrature?
 - Retro-pro excitation v.s. light ring crossing time?
 - Overtone $n>5$ fitting in the global sense?
 - Data strategy of waveform stacking? ↗

Summary and outlook

- Towards a more complete test of GR
 - QNM temporal-spatial fitting
 - S/Y distinguishability
 - Retrograde excitations
- BH spectroscopy conclusions reinforced
 - Higher-order (l,m) modes
 - Overtones
- Outlook
 - Spin misaligned cases? Mass/current quadrature?
 - Retro-pro excitation v.s. light ring crossing time?
 - Overtone $n>5$ fitting in the global sense?
 - Data strategy of waveform stacking? ↗

Early excitation of retrograde modes



G0: Why do the **retrograde modes** also play roles in fitting **spin-aligned binaries**, and are excited even **earlier** than prograde mode? **Light ring crossing?** Overfitting?

Future waveform stacking strategy

**Thanks!
Q & A**

Xiang Li (xiangli@caltech.edu)

34

